RF AND SPACE-CHARGE INDUCED EMITTANCES IN LASER-DRIVEN RF GUNS

Kwang-Je Kim*

Lawrence Berkeley Laboratory, 1 Cyclotron Road, Berkeley, CA 94720

Yu-Jiuan Chen**

Lawrence Livermore National Laboratory, P.O. Box 808, Livermore, CA 94550

I. Introduction

Laser-driven rf electron guns[1] are potential sources of high-current, low-emittance, short bunch-length electron beams, which are required for many advanced accelerator applications, such as free-electron lasers and injectors for high-energy machines. In such guns the design of which was pioneered at Los Alamos National Laboratory[1] and which is currently being developed at several other laboratories,[2,3,4] a high-power laser beam illuminates a photo-cathode surface placed on an end wall of an rf cavity. The main advantages of this type of gun are that the time structure of the electron beam is controlled by the laser, eliminating the need for bunchers, and that the electric field in rf cavities can be made very strong, so that the effects due to space-charge repulsion can be minimized. In this paper, we present an approximate but simple analysis for the transverse and longitudinal emittances in rf guns that takes into account both the time variation of the rf field and the space-charge effect. The results are compared and found to agree well with those from simulation. In the following, we review the theory[5] in Sections II and III, and the simulation results[6] in Section IV.

II. Analysis of RF Effects[5]

The structure of a rf gun cavity is schematically illustrated in Fig. 1. The cavity consists of $(\frac{1}{2} + n)$-cells, the first cell being a half-cell so that electrons see the maximum accelerating field as they are emitted from the cathode. The accelerating field in the cavity will be assumed to be of the following simple form:

$$E_z = E(z) \cos kz \sin (\omega t + \phi_0); \quad E(z) = E_0 \theta(z_f - z) \ . \tag{1}$$

Here λ is the rf wavelength, $k = 2\pi/\lambda$, c is the velocity of light, $\omega = ck$, ϕ_0 is the rf phase as the electron leaves the cathode (located at $z = 0$) at $t = 0$, E_0 is the peak accelerating field, θ is the step function, and $z_f = (n + \frac{1}{2})\lambda/2$ is the location of the cavity exit. When E_z is independent of transverse coordinates, the transverse fields are linear in transverse coordinates and are given by

$$E_r = -\frac{r}{2}\frac{\partial}{\partial z}E_z \ , \ cB_\theta = \frac{r}{2c}\frac{\partial}{\partial t}E_z \ . \tag{2}$$

Here r and θ are the cylindrical coordinates. The fields, Eq. (1) and Eq. (2), can be considered as a π-mode excitation of an ideal cavity.[2]

The equations for rf acceleration for $z < z_f$ are

$$\frac{d\gamma}{dz} = \frac{eE_0}{2mc^2}[\sin (\phi) + \sin (\phi + 2kz)] \ , \tag{3}$$

Photo cathode surface

$\vdash \lambda/4 \dashv \vdash \ \lambda/2 \ \dashv \vdash \ \lambda/2 \ \dashv$
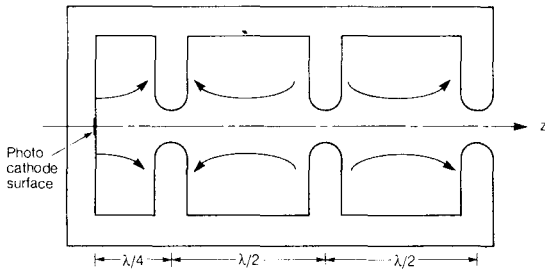
Fig. 1. Schematics of the rf laser gun.

$$\frac{d\phi}{dz} = k\left[\frac{\gamma}{\sqrt{\gamma^2 - 1}} - 1\right] \ . \tag{4}$$

Here γ is the electron energy in units of its rest energy and $\phi = \omega t - kz + \phi_0$. Near the cathode where $kz \ll \phi$, it follows from Eq. (3) that

$$dz \approx \frac{1}{2\alpha k \sin \phi_0} d\gamma \ , \tag{5}$$

where

$$\alpha = eE_0/2mc^2k \tag{6}$$

is a dimensionless parameter representing the acceleration gradient.

An approximate solution of Eqs. (3) and (4) can be obtained based on the fact that the RHS of Eq. (4) is significantly different from zero in the region where the electrons are still nonrelativistic, i.e., near the cathode surface. The result is that, at the exit of the $(\frac{1}{2} + n)$-cell cavity, the phase ϕ approaches the value

$$\phi_f = \frac{1}{2\alpha \sin \phi_0} + \phi_0 \ , \tag{7}$$

and the electron energy becomes

$$\gamma_f = 1 + \alpha [(n + \frac{1}{2}) \pi \sin \phi_f + \cos \phi_f] \ . \tag{8}$$

The force in the radial direction is given by $F_r = e(E_r - \beta cB_\theta)$, which, using Eqs. (1) and (2), can be written in the following form:

$$F_r = er\left\{ -\frac{1}{2c}\frac{d}{dt}\left[E(z) \sin kz \cos (\omega t + \phi_0)\right] - \frac{1}{2}\left[\frac{d}{dz}E(z)\right] \sin \phi \right.$$
$$\left. + \frac{(\beta - 1)}{2}\left[\frac{d}{dz}E(z)\right] \sin kz \cos (\omega t + \phi_0)\right\} \ . \tag{9}$$

The transverse momentum is obtained by integrating Eq. (9) with respect to time t. We assume that the transverse deflection is small so that the radius r can be regarded as constant. The first term in the above is a total derivative of an expression that vanishes at the cathode surface and outside the cavity, thus its contribution to the transverse momentum vanishes. The contribution from the third term is small because of the $(\beta - 1)$-factor. Thus the main contribution comes from the second term, which is important only in the region where $dE(z)/dz$ is non-vanishing, i.e., near the cavity exit. With E(z) given by the step function (see Eq. (1)), the dimensionless transverse momentum at the cavity exit in the Cartesian coordinate, $p_x = \beta\gamma x'$, where x' is the angle in the x-direction, becomes

$$p_x = (\alpha k \sin \phi_f)x \ . \tag{10}$$

Equations (8) and (10) are the basis for our discussion of the rf-induced emittances. The phase ϕ_f varies over the length of the electron bunch, $\phi_f = \langle\phi_f\rangle + \Delta\phi; \ \Delta\phi = -k\Delta z$, where $\langle\phi_f\rangle$ is the average phase. Thus the transverse phase-space distribution consists of a collection of lines with different slopes corresponding to different $\Delta\phi$, as illustrated in Fig. 2. The normalized transverse emittance is defined as[7]

$$\varepsilon_x = \sqrt{\langle p_x^2\rangle \langle x^2\rangle - \langle p_x x\rangle^2} \ , \tag{11}$$

where the angular brackets refer to the average values. Assuming that the electrons' density distribution is Gaussian, with rms transverse and longitudinal lengths given respectively by σ_x and σ_z, we find from Eqs. (9) and (11) that the emittance is at a minimum for $\langle\phi_f\rangle = \pi/2$ and

$$\varepsilon_x^{rf} = \alpha k^2 \sigma_x^2 \sigma_z |\cos \langle\phi_f\rangle| \ ; \ \langle\phi_f\rangle \neq \pi/2 \ , \tag{12}$$

$$\varepsilon_x^{rf} = \alpha k^3 \sigma_x^2 \sigma_z^2/\sqrt{2} \ ; \ \langle\phi_f\rangle = \pi/2 \ . \tag{13}$$

In the above, the superscript rf refers to the fact that we are considering the rf-induced effects.
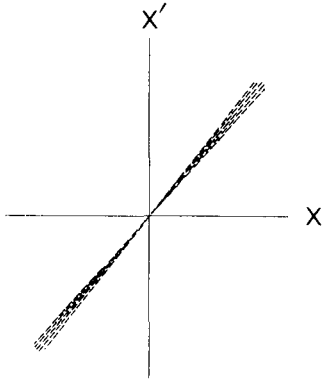
Fig. 2. Electron distribution in transverse phase space due to time-dependent focusing of the rf field.

The longitudinal emittance is defined as

$$\epsilon_z = \sqrt{\langle(\Delta p_z)^2\rangle\langle(\Delta z)^2\rangle - \langle\Delta p_z \Delta z\rangle^2} \ , \qquad (14)$$

where $\Delta p_z = \Delta(\beta\gamma) \approx \Delta\gamma$ for the relativistic case $\beta \approx 1$. We write $\gamma_f = \langle\gamma_f\rangle + \Delta\gamma$, and expand Eq. (8) in $\Delta\phi = -k\Delta z = \phi_f - \langle\phi_f\rangle$. Setting $\langle\phi_f\rangle = \pi/2$ to minimize the transverse emittance, we obtain

$$\Delta\gamma = \alpha k\Delta z - \frac{1}{2}\left[\langle\gamma_f\rangle - 1\right]k^2(\Delta z)^2 - \frac{\alpha k^3}{3!}(\Delta z)^3 + \cdots \ . \qquad (15)$$

The nonlinear terms in the above contribute to the longitudinal emittance, and one obtains to the lowest order

$$\epsilon_z^{rf} = \sqrt{3}\left[\langle\gamma_f\rangle - 1\right]k^2\sigma_z^3 \ . \qquad (16)$$

III. Analysis of the Space-Charge Effects[5]

A repulsive force attributable to space charge causes the emittance to increase. To study this effect, we assume that all electrons are moving with the same velocity, v, in the z-direction. In the reference frame moving with the electrons, the electromagnetic interaction is completely described by a purely electrostatic field E'. The field components in the laboratory frame which give rise to the x- and z-components of the force are given by the Lorentz transformation $E_x = \gamma E_x'$, $B_y = \gamma(\beta/c)E_x'$, $E_z = E_z'$. Here, B_y is the magnetic field. The components of the force are

$$F_x = e(E_x - vB_y) = \frac{e}{\gamma}E_x' \ , \ F_z = eE_z' \ . \qquad (17)$$

In the following, we assume the charge distribution to be cylindrically symmetric, so that we do not need to consider F_y separately. It can be shown that the force given by Eq. (17) vanishes as γ^{-2} for $\gamma \gg A$, where $A = \sigma_x/\sigma_z$ is the aspect ratio. Thus we can write $E = f(\gamma)/\gamma^2$, where $f(\gamma)$ is a function slowly varying in γ for $\gamma \gg A$. The contribution to the dimensionless momentum due to the space-charge force is given by

$$(p_x, p_y, \Delta p_z) \equiv p = \frac{1}{mc^2}\int\frac{1}{\gamma^2\beta}f(\gamma)\,dz \ . \qquad (18)$$

We evaluate Eq. (18) approximately by noting that the factor $1/\gamma^2\beta$ in the integrand decreases rapidly as γ becomes large. Thus we replace $f(\gamma)$ by $f(1)$ and dz by Eq. (5). The result is $p = (\pi/2)(1/E_0 \sin\phi_0)E^{sc}$, where E^{sc} is the electrostatic field due to the charge distribution at rest in the laboratory frame. From this and from Eqs. (11) and (14), we obtain the space-charge induced emittances as follows:

$$\epsilon_i^{sc} = \frac{\pi}{4}\frac{1}{\alpha k}\frac{1}{\sin\phi_0}\frac{I}{I_A}\mu_i(A) \ ; \ i = x \text{ or } z \ , \qquad (19)$$

where I is the peak current, $I_A = 17{,}000$ Amp known as the Alfvén current, and the functions $\mu_i(A)$ are defined in terms of the normalized field $\mathcal{E}_i = (4\pi\epsilon_0/n_0)E_i^{sc}$ (n_0 = the line density) by

$$\mu_x(A) = \sqrt{\langle\mathcal{E}_x^2\rangle\langle x^2\rangle - \langle\mathcal{E}_x\cdot x\rangle^2} \ , \ \mu_z(A) = \sqrt{\langle\mathcal{E}_z^2\rangle\langle\Delta z^2\rangle - \langle\mathcal{E}_z\cdot\Delta z\rangle^2} \ . \qquad (20)$$

Note that $\mu_i(A)$, being dimensionless, are functions of A only. For the Gaussian charge distribution, these functions are approximately given by

$$\mu_x(A) \sim \frac{1}{3A + 5} \ , \ \mu_z(A) = \frac{1.1}{1 + 4.5A + 2.9A^2} \ . \qquad (21)$$

How do the rf-induced and the space-charge induced emittance add? It turns out that there are correlations between those two effects so that the total emittance ϵ_i is given by

$$\sqrt{(\epsilon_i^{rf})^2 + (\epsilon_i^{sc})^2} < \epsilon_i < \epsilon_i^{rf} + \epsilon_i^{sc} \ . \qquad (22)$$

A more detailed derivation of the results in Sections II and III, as well as the application of these results to the case where the electron distribution is uniform in a cylinder, can be found in Ref. 5.

IV. Comparison with Simulations[6]

The program PARMELA, modified by McDonald to include the emission of electrons from a photocathode by a laser pulse,[2] has been used to simulate the beam dynamics in the laser-driven rf guns. We have studied a $(\frac{1}{2} + 2)$-cell, 1269 MHz, $E_0 = 30$ MV/m cavity, generating 1 nC, $\sigma_t = \sigma_z/c = 6$ ps bunches. The laser spot size is $\sigma_x = 3$ mm. These are the parameters for a possible high-brightness gun for an LBL-LLL-SLAC collaboration.[3]

First, the space-charge interaction is turned off in the simulation to study the rf effects alone. In this simulation we use the simple rf field configuration given by Eqs. (1) and (2). In comparing Eq. (7) with simulation, it is found that the exit phase ϕ_f from theory and from simulation agree within 10% for $\phi_0 \geq 30°$. Note that the theory is not expected to be valid for a small value of $\sin\phi_0$.

The transverse emittance ϵ_x^{rf} versus ϕ_0 (at the center of the electron bunch) is presented in Fig. 3. We see that the optimized emitting phase ϕ_0 from simulation is smaller by 7° than that predicted by theory (obtained by setting $\phi_f = 90°$ in Eq. (7)). If the two curves in Fig. 3 are shifted relative to each other so that their minima coincide, then ϵ_x^{rf} from the simulation is about twice as large as that from the theory. The discrepancy seems due to the fact that the bunch radius is assumed to be constant in deriving Eqs. (12) and (13); in simulation, it is found that the bunch radius increases by about a factor of 1.5 as the bunch travels from the cathode to the cavity exit. Note that the emittance given by Eqs. (12) and (13) is proportional to σ_x^2. The σ_x^2-dependence of the transverse emittance agrees well with simulation results using different values for σ_x.

The longitudinal emittance σ_z^{rf} from simulation agrees with that predicted by theory (Eq. (6)) within a factor of two. When the emitting phase ϕ_0 corresponds to the minimum transverse emittance, $\phi_0 = 58°$, the agreement is even better. Figure 4 compares ϵ_z^{rf} obtained from the simulation with that from the theory for different values of the laser pulse length σ_t for $\phi_0 = 58°$.

The effects due to the nonlinearity of the rf field in a practical cavity design is checked by comparing the results of PARMELA runs using a linear rf field given by Eqs. (1) and (2), with those using the rf field calculated by SUPERFISH based on a cavity geometry similar to the BNL design.[2] The effect of the nonlinearity on the transverse emittance is found to be small. However, electrons gain more energy in the rf field calculated by SUPERFISH.

The emittance growth due to the space-charge effect is studied by calculating the total emittance ϵ_i including the space-charge interaction in
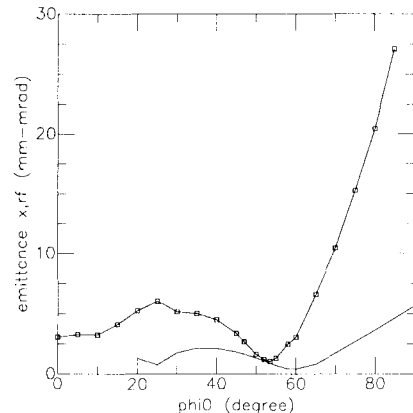
Fig. 3. The rf induced transverse emittance as a function of ϕ_0 calculated from simulation (marked by □) and from theory (solid line).
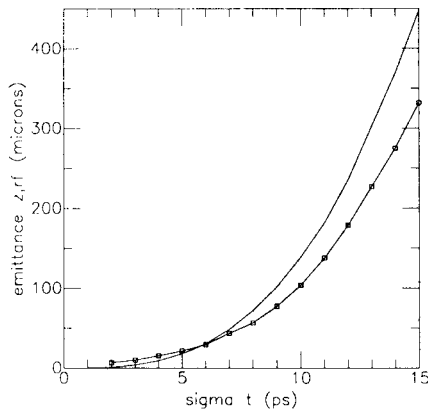
Fig. 4. The rf induced longitudinal emittance as a function of σ_t calculated from simulation (marked by □) and from theory (solid line).
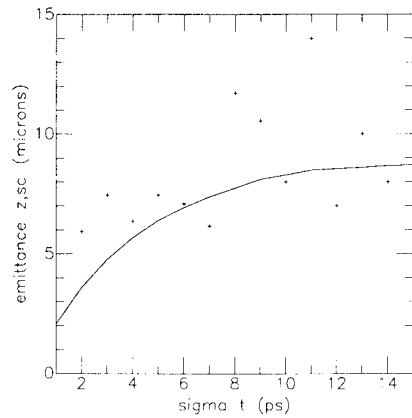
Fig. 6. The space-charge induced longitudinal emittance calculated from simulation (marked by +) and from theory (solid line).

the simulation. The space-charge induced transverse emittance ε_x^{sc} is estimated in two ways — by using $\varepsilon_x = \sqrt{(\varepsilon_x^{rf})^2 + (\varepsilon_x^{sc})^2}$ and by using $\varepsilon_x = \varepsilon_x^{rf} + \varepsilon_x^{sc}$. The results are compared with theoretical prediction, Eqs. (19) and (21), in Fig. 5. We see that the ε_x^{sc} from theory agrees more or less within the two curves obtained from simulation. The longitudinal space-charge induced emittance ε_z^{sc} is estimated from the simulation data by using $\varepsilon_z = \varepsilon_z^{sc} + \varepsilon_z^{rf}$, and compared with the theoretical prediction in Fig. 6. There is a large scattering of the simulation results. This is due to the fact that the longitudinal emittance is dominated by the rf effect in the case under consideration. Nevertheless, the agreement between the theory and the simulation is encouraging. Finally we remark that ε_z^{sc} calculated from the simulation data using $\varepsilon_z = \sqrt{(\varepsilon_z^{rf})^2 + (\varepsilon_z^{sc})^2}$ shows a wider scattering and is generally larger than those shown in Fig. 6.

A more detailed report of the simulation results can be found in Ref. 6.
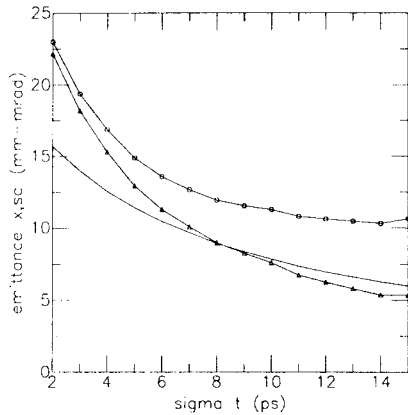
Fig. 5. The space-charge induced transverse emittance calculated from simulation using $\varepsilon_z = \sqrt{(\varepsilon_z^{rf})^2 + (\varepsilon_z^{sc})^2}$ (marked by □), using $\varepsilon_z = \varepsilon_z^{rf} + \varepsilon_z^{sc}$ (marked by Δ) and from theory (solid line).

References

1. J.S. Fraser et al., "Photocathodes in Accelerator Applications," Proc. 1987 IEEE Particle Accelerator Conference, IEEE Cat. No. 87CH.2387-9, 1705 (March, 1987).

2. K.T. McDonald, "Design of the Laser-Driven RF Electron Gun for the BNL Accelerator Test Facility," Princeton Preprint DOE/ER/3072-43 (March, 1988); submitted to IEEE trans. on Electron Devices.

3. S. Chattopadhay et al., "Conceptual Design of a Bright Electron Injector based on a Laser-Driven Photo-Cathode RF Gun," paper submitted to 1988 Linear Accelerator Conference.

4. H. Chaloupka et al., "A Proposed Super Conducting Photoemission Source of High Brightness," paper submitted to the European Particle Accelerator Conference, Rome, Italy (June 7–11, 1988).

5. K.-J. Kim, "RF and Space-Charge Effects in Laser-Driven RF Electron Guns," LBL-25807 (August, 1988); submitted for publication to Nucl. Inst. Methods.

6. Y.-J. Chen, "Simulations of High-Brightness RF Photocathode Guns for LLNL-SLAC-LBL 1 GeV Test Experiment," LLNL pub. UCRL-99675 (August, 1988).

7. P.M. Lapostolle, "Possible Emittance Increase Through Filamentation Due to Space Charge in Continuous Beam," IEEE Trans. Nucl. Sci. 18, 1101 (1971).